Plastic model for asymmetrically loaded reinforced concrete slabs

Lantsoght, Eva; van der Veen, Cor; de Boer, A.

Citation (APA)
Lantsoght, E., van der Veen, C., & de Boer, A. (2017). Plastic model for asymmetrically loaded reinforced
concrete slabs. In M. Mahamid, & M. Shin (Eds.), *Symposium volume: Recent Developments in Two-Way
Slabs: Design, Analysis, Construction, and Evaluation: An ACI Technical Publication* (Vol. SP-321, pp. 1.1-
1.20). Article SP-321—1 ACI.

Important note
To cite this publication, please use the final published version (if applicable).
Please check the document version above.

Plastic model for asymmetrically loaded reinforced concrete slabs

Eva O. L. Lantsoght, Cor van der Veen and Ane de Boer

Synopsis: Most methods for the design and analysis of reinforced concrete slabs for punching are based on experiments on slab-column connections, reflecting the situation in building slabs. Slab-column connections with unbalanced moments have also been studied in the past. Experiments indicate that the accuracy of models for asymmetrically loaded slabs is lower than for symmetrically loaded slabs. In this paper, the difference in accuracy between test predictions for symmetrically and asymmetrically loaded slabs is tackled. A plastic model, the Extended Strip Model, is proposed. The results of maximum loads according to this model are compared to experimental results of symmetrically and asymmetrically loaded slabs. The comparison between the proposed Extended Strip Model and the experimental results shows that the model has a consistent performance for both symmetrically and asymmetrically loaded slabs. Moreover, the model has as an advantage that it combines the failure modes of flexure, shear and punching. The proposed model can be used for the analysis of slabs. In particular, it can be used for the assessment of existing slab bridges subjected to concentrated live loads.

1 ACI member **Eva O. L. Lantsoght** is an assistant professor at Universidad San Francisco de Quito, Ecuador and a
2 researcher at Delft University of Technology, The Netherlands. She is a member of ACI Sub-Committee 445-0D
3 Shear & Torsion – Shear Databases, and an associate member of ACI Committee 342, Evaluation of Concrete
4 Bridges and Bridge Elements, and Joint ACI-ASCE Committees 421, Design of Reinforced Concrete Slabs and 445,
5 Shear and Torsion.
6
7 **Cor van der Veen** is an associate professor at Delft University of Technology, Delft, The Netherlands. He received
8 his M.Sc. and Ph.D. from Delft University of Technology. He is a member of various National Committees. His
9 research interests include (very) high strength (steel fiber) concrete, concrete bridges and computational mechanics.
10
11 **Ane de Boer** is a senior advisor at Rijkswaterstaat, the Ministry of Infrastructure and the Environment, Utrecht, The
12 Netherlands. He received his MSc and PhD from Delft University of Technology. He is a member of some National
13 Committees, *fib* Special Activity Group 5 and member of an IABSE Working Committee. His research interests are
14 remaining lifetime, existing structures, computational mechanics, traffic loads and composites.
15
16
17   INTRODUCTION
18   Because of constraints in space and available loading, punching of slabs is typically studied with slab-column
19 connections (ASCE-ACI Task Committee 426, 1974). This type of test setup reflects the situation in building slabs.
20 As a result, the available code equations are either (semi-)empirical methods derived from a statistical analysis of
21 slab-column connection tests, or based on mechanical models, verified with slab-column connection tests.
22   For the one-way shear capacity of beams, the situation is similar. Experiments are typically carried out on
23 small, slender, heavily reinforced concrete beams tested in three- or four-point bending (Reineck et al., 2013). The
24 available code equations are either (semi-)empirical methods derived from a statistical analysis of these tests, or
25 based on mechanical models and verified with the available tests.
26   When the shear capacity of reinforced concrete slab bridges is assessed, both the beam shear (one-way shear)
27 and punching shear (two-way shear) capacity under the combination of distributed dead loads and the prescribed
28 live loads (typically distributed lane loads and concentrated loads from the design truck or tandem) need to be
29 verified. This loading situation is different from a slab-column connection or simplified beam shear test setup, and is
30 an asymmetrical loading situation because of the different positions of the design trucks or tandems over the lanes.
31   An asymmetrical loading condition that is studied for building slabs is the case of slab-column connections
32 with unbalanced moments (Barzegar et al., 1991), reflecting the loading situation at edge and corner columns. The
33 unbalanced moment is then considered to cause a contribution to the occurring shear stresses on the punching
34 perimeter that needs to be summed with the direct shear stress on the punching perimeter, and the code methods
35 reflect this approach.
36
37   RESEARCH SIGNIFICANCE
38   The presented study considers the shear capacity of symmetrically and asymmetrically loaded reinforced
39 concrete slabs. Traditionally, the shear capacity is considered as the one-way shear capacity and the two-way shear
40 capacity separately. In this paper, a plastic model is described, the Extended Strip Model, and the applicability to
41 both symmetrically and asymmetrically loaded reinforced concrete slabs is highlighted. Experimental results show
42 the validity of the presented model.
43
44   LITERATURE REVIEW
45 Existing methods for the shear capacity of slabs
46   One-way shear models — The shear capacity of beams without transverse reinforcement (the situation that
47 occurs when considering the one-way shear capacity of slabs) has been fiercely debated over the past century, and a
48 multitude of (semi-)empirical and mechanical models have been developed. The code provisions, which result from
49 semi-empirical models based on a statistical analysis, will be discussed in the next section. In this section,
50 mechanical models are discussed.
51   The first approach is the Modified Compression Field Theory (Vecchio and Collins, 1986), which has been
52 adopted into the Canadian building provisions CSA A23.3 (Canadian Standards Association, 2004), AASHTO
53 LRFD Code (AASHTO, 2015) and the *fib* Model Code (fib, 2012), replacing in these codes the semi-empirical
54 formulations with a mechanical model for the first time. In the Modified Compression Field Theory and the
55 Simplified Modified Compression Field Theory (Bentz et al., 2006), the constitutive relations of cracked concrete
56 are used, based on average stresses and strains. For members without transverse reinforcement, concrete tension ties

resulting from aggregate interlock action are used (Adebar and Collins, 1996). These equations were derived from testing concrete panels subjected to in-plane shear and axial stresses in a panel tester (Collins et al., 1996), instead of testing beams in shear, and the resulting method has shown to lead to good results when verified in beam shear tests (Collins et al., 2015). Models that are based on the same principle are fixed-angle softened-truss models and rotating-angle softened-truss models (Hsu, 1996).

A second approach is the Critical Shear Crack Theory (Muttoni and Schwartz, 1991), which has been developed for both one-way and two-way shear. The basic assumption of this theory is that the shear strength of members without transverse reinforcement is governed by the width and roughness of a shear crack, which develops through the inclined compression strut carrying the shear. For one-way shear, the failure criterion is based on the proportionality between the width of the critical shear crack and the strain at a control depth (Muttoni and Ruiz, 2008). The width of the critical shear crack is considered to be influenced by the aggregate size and the spacing between the layers of reinforcement.

A third family of approaches are based on the theory of plasticity. Models based on the lower bound theorem of plasticity are strut-and-tie models (Schlaich et al., 1987). For the application to one-way shear in members without transverse reinforcement, concrete tension ties need to be developed based on the mechanisms of shear transfer (Reineck, 2010). For this case, a combination of the effect of aggregate interlock, dowel action, and residual tension across the crack can be considered. Models based on the upper bound theorem of plasticity consider a mechanism, consisting of yield lines and/or plastic hinges. For shear, the yield line of a critical shear crack can be studied (Nielsen and Hoang, 2011).

A fourth family of approaches study the shear transfer mechanisms on a so-called "concrete tooth". The tooth is the part between two flexural cracks, which looks like a concrete cantilever fixed in the compression zone and loaded by horizontal forces resulting from bond (Kani, 1964). These models also showed for the first time that shear transfer can be separated into beam shear and arching action, and used this observation to explain the experimentally observed "valley of diagonal failure."

A final group of methods is based on fracture mechanics, and study both stress-strain relations as well as tensile stress-crack opening relations (Niwa, 1997). The failure criterion is then related to tensile stresses, and expressed as a function of the maximum aggregate size and the fracture energy (Walraven, 2007). A model (Gastebled and May, 2001) based on the assumption that the release of the main reinforcement by splitting controls the opening and extension of the diagonal crack was developed. According to this model, once splitting has started, the reinforcement bar loses its bond with the concrete, reducing the tensile stiffness, and resulting in opening and extending of the diagonal crack. Then, the fundamental relation of fracture mechanics is used to describe a splitting failure.

Two-way shear models — The mechanics behind two-way shear have been a popular research topic over the past century. The same mechanisms of shear transfer occur as for one-way shear, but the situation is even more complex as a result of the combined flexural and diagonal tensile cracking and the three-dimensional nature of the problem (Park and Gamble, 2000). Virtually all experimental results of punching tests have been executed on slab-column connections, where the slab is not extended past its line of contraflexure. When extending these results to bridge deck slabs subjected to concentrated wheel loads, it must be noted that the principal shear forces and moments are not rotationally symmetric (Rombach and Latte, 2009).

A first group of punching models are based on limiting the shear stress on a critical perimeter. These models are used in most design codes. The shape of the punching perimeter is determined by taking a certain distance away from the loaded area. This distance is based on experimentally observed punching failure cones. However, it is known (Menétrey, 2002) that the angle of inclination is mostly a function of the interaction between shear and flexure. Angles of 30° indicate predominantly shear failures and angles of 90° indicate pure flexure. The models from Eurocode 2 and ACI 318-14, which will be discussed in the next section, are based on limiting the shear stress on a critical perimeter.

A second group are plasticity-based models. Three-dimensional strut-and–tie models are available (Alexander and Simmonds, 1987), yet experiments showed that the compressive arches are curved instead of straight. Therefore, the Bond Model or Strip Model (Alexander and Simmonds, 1992) was developed. This model combines arching action in strips extending from the column, a limiting one-way shear on the interface between strips and slab quadrants, and two-way flexure inside slab quadrants. The Strip Model was developed for concentric punching shear, but has been extended to asymmetric loading situations with the Extended Strip Model (Lantsoght et al., (in review)). The Extended Strip Model will be discussed later in this paper. A model based on the upper bound theorem of plasticity, studying the slab portion outside the shear crack and bound by this crack, radial cracks, and the line of contraflexure, is available as well (Kinnunen and Nylander, 1960). Over the past years, this model

1 has been extended and improved, among others by using a failure criterion based on fracture mechanics (Hallgren,
2 1996), and by incorporating compressive membrane action (Wei, 2008).
3   As mentioned with the one-way shear models, the Critical Shear Crack Theory is also suitable for two-way
4 shear. For two-way shear, the width of the critical shear crack is considered a function of the slab rotation (Muttoni,
5 2008). The two-way shear approach from the Critical Shear Crack Theory is implemented in the *fib* Model Code
6 2010 (fib, 2012). The method can be extended for asymmetric loading conditions without changing the failure
7 criterion, but the load-rotation relationship for that situation should then be derived by integration of the moment-
8 curvature relation of the slab. The shear stresses on the perimeter will also not be uniform, with certain parts of the
9 perimeter reaching their limiting stress before other parts (Sagaseta et al., 2011), and the stresses along the perimeter
10 need to be integrated. For complex situations, such as reinforced concrete slab bridges subjected to concentrated
11 wheel loads, non-linear finite element models are necessary to determine the load-rotation relationship of the slab
12 (Falbr, 2011). The method then requires significant computational time and power.
13   Because of the complex mechanics of punching, often finite element models are used. These models range
14 from simple elastic plate models to sophisticated nonlinear models that account for discrete cracks and describe the
15 nonlinear behavior of the materials. The *fib* Model Code (fib, 2012) describes the use of finite element models as the
16 highest Level of Approximation for punching. Further research (Belletti et al., 2015) showed that a combination of a
17 crack model and a model consisting of layers of shells can be combined with the Critical Shear Crack Theory (as
18 described in the *fib* Model Code) to reach the highest Level of Approximation, and to determine both the shear and
19 flexural capacities of the studied structural element.
20   Beam analogy methods (Park and Gamble, 2000) have also been developed for punching. These models
21 require the study of slab strips (beams) subjected to bending moment, torsional moment, and a shear force,
22 combined with redistribution between the strips. The large number of possible limiting strength combinations makes
23 these methods time-consuming and confusing.
24
25 <u>Code provisions</u>
26   <u>Eurocode 2</u> — The beam shear (one-way shear) provisions from NEN-EN 1992-1-1:2005 (CEN, 2005) are
27 semi-empirical formulas. Since slab bridges do not have stirrups, only the shear resistance of structural members
28 without stirrups is discussed here. This shear resistance is determined as follows:

$$V_{Rd,c} = \left(C_{Rd,c} k \left(100 \rho_l f_{ck} \right)^{1/3} + k_1 \sigma_{cp} \right) b_w d_l \geq \left(v_{min} + k_1 \sigma_{cp} \right) b_w d_l \tag{1}$$

$$k = 1 + \sqrt{\frac{200}{d_l}} \leq 2.0 \tag{2}$$

31 with:
32 $V_{Rd,c}$ the design shear capacity in [kN];
33 k the size effect factor, with d_l in [mm];
34 ρ_l the flexural reinforcement ratio;
35 f_{ck} the characteristic cylinder compressive strength of the concrete in [MPa];
36 k_1 0.15;
37 σ_{cp} the axial stress on the cross-section in [MPa];
38 b_w the web width of the section in [m];
39 d_l the effective depth to the main flexural reinforcement in [mm].
40 According to the Eurocode procedures, the values of $C_{Rd,c}$ and v_{min} may be chosen nationally. The default values are
41 $C_{Rd,c} = 0.18/\gamma_c$ with $\gamma_c = 1.5$ in general and v_{min} (f_{ck} in [MPa]):

$$v_{min} = 0.035 k^{3/2} f_{ck}^{1/2} \text{ in [MPa]} \tag{3}$$

43 NEN-EN 1992-1-1:2005 §6.2.2 (6) accounts for the influence of the shear span to depth ratio on direct load transfer.
44 The contribution of a load applied within a distance $0.5 d_l \leq a_v \leq 2 d_l$ from the edge of a support to the shear force V_{Ed}
45 may be multiplied by the reduction factor $\beta = a_v / 2 d_l$. In that clause of the code, the distance a_v is considered as the
46 distance between the face of the load and the face of the support, or the center of the support for flexible supports.
47   The punching shear (two-way shear) provisions from NEN-EN 1992-1-1:2005 (CEN, 2005) follow a
48 similar format as the beam shear provisions. The design punching shear capacity is calculated as follows:

$$v_{Rd,c} = C_{Rd,c} k \left(100 \rho_l f_{ck} \right)^{1/3} + k_1 \sigma_{cp} \geq v_{min} + k_1 \sigma_{cp} \tag{4}$$

50 with
51 $\rho_l = \sqrt{\rho_{lx} \times \rho_{ly}} \leq 0.02$ the geometric reinforcement ratio;

1   ρ_{lx}, ρ_{ly} relate to the bonded tension steel *x*- and *y*-directions respectively. The values ρ_{lx} and ρ_{ly} should be calculated
2   as mean values taking into account a slab width equal to the column width plus *3d* each side.
3   All other parameters are determined in the same way as for the one-way shear provisions.
4   The shear stress v_{Ed} (in [MPa]) on the perimeter should not exceed $v_{Rd,c}$. The stress v_{Ed} can be calculated in a
5   simplified manner as:

6
$$v_{Ed} = \beta_{pu} \frac{V_{Ed}}{u_i d} \tag{5}$$

7   with
8   V_{Ed} the shear force in [kN];
9   u_i the perimeter of the critical section in [m];
10   d the effective depth, determined as the average of the effective depth to the longitudinal reinforcement and
11   the effective depth to the transverse reinforcement, in [mm];
12   β_{pu} a correction factor, approximate values are:
13   internal column: $\beta_{pu} = 1.15$;
14   edge column: $\beta_{pu} = 1.4$;
15   corner column: $\beta_{pu} = 1.5$.
16   A more detailed method for asymmetric loading conditions determines v_{Ed} as follows:

17
$$v_{Ed} = \frac{V_{Ed}}{u_i d}\left(1 + k_{pu} e_{pu} \frac{u_i}{W}\right) \tag{6}$$

18   with
19   k_{pu} a parameter, equal to 0.6 when the column has a square cross-section;
20   e_{pu} the eccentricity ratio, determined by the eccentricity between the center of the load and the center of gravity
21   of the area within the perimeter;
22   W corresponds to a distribution of shear on the punching parameter, which can be determined for a
23   rectangular column as:

24
$$W = \frac{c_1^2}{2} + c_1 c_2 + 4c_2 d + 16d^2 + 2\pi d c_1 \tag{7}$$

25   with
26   c_1 the column dimension parallel to the eccentricity of the load;
27   c_2 the column dimension perpendicular to the eccentricity of the load.
28   It should be noted that the determination of e_{pu} is an approximation, and that, to determine the true
29   eccentricity, a nonlinear finite element analysis should be carried out. The eccentricity should then be determined as
30   the ratio of the design moment M_{Ed} and the design shear force V_{Ed}.
31   The critical perimeter is taken at *2d* from the loaded area. Around rectangular loaded areas, rounded
32   corners are used for the perimeter. For loads close to the support (within a distance $0.5d \leq a_v \leq 2d$), the design shear
33   capacity can be increased with $2d/a_v$, and the perimeter u_i is based on the distance a_v instead of a distance $2d$. Eq. (7)
34   for loads close to the support (within a distance $0.5d \leq a_v \leq 2d$), becomes:

35
$$W = \frac{c_1^2}{2} + c_1 c_2 + 2c_2 a_v + 4a_v^2 + \pi a_v c_1 \tag{8}$$

36
37   <u>ACI 318-14</u> — The beam shear (one-way shear) provisions from ACI 318-14 (ACI Committee 318, 2014)
38   are also semi-empirical formulas. The shear capacity V_c in [kN] is determined for normal weight concrete ($\lambda = 1$) as
39   follows (in SI-units, f_c' in MPa, 1 MPa = 145 psi):

40
$$V_c = \left(0.16\sqrt{f_c'} + 17\rho_l \frac{V_u d_l}{M_u}\right)b_w d_l \leq \left(0.16\sqrt{f_c'} + 17\rho_l\right)b_w d_l \leq 0.29\sqrt{f_c'}b_w d_l \tag{9}$$

41   with

42   f_c' the specified concrete compressive strength in [MPa], and the limit of $\sqrt{f_c'}$ is 100 psi (8.3 MPa);

43   ρ_l the longitudinal reinforcement ratio;
44   V_u the sectional shear force in [kN];
45   M_u the sectional moment; where M_u occurs simultaneously with V_u at the section considered in [kNmm];

1. d_l the effective depth to the longitudinal reinforcement in [mm];
2. b_w the web width in [m].
3. ACI 318-14 recommends the use of nonlinear analysis or strut-and-tie models for members with concentrated loads
4. within a distance twice the member depth from the support.
5.   Likewise, the punching shear (two-way shear) provisions from ACI 318-14 are semi-empirical formulas.
6. The nominal punching shear capacity V_c in [kN] for normal weight concrete ($\lambda = 1$) is determined as follows (in SI-
7. units, f_c' in MPa, 1 MPa = 145 psi):

8.
$$V_c = \min \begin{cases} \left(0.166 + \dfrac{0.333}{\beta_{pun}}\right)\sqrt{f_c'}\,b_o d \\[2ex] \left(\dfrac{\alpha_s d}{b_o} + 0.166\right)\sqrt{f_c'}\,b_o d \\[2ex] 0.333\sqrt{f_c'}\,b_o d \end{cases} \tag{10}$$

9. with
10. β_{pun} the ratio of the long side to the short side of the column, concentrated load or reaction area;
11. b_o the perimeter of the critical section for shear, taken at a distance $d/2$ away from the periphery of the loaded
12.   area, in [m];
13. α_s 40 for interior columns, 30 for edge columns, 20 for corner columns;
14. d the average of the effective depth to the longitudinal reinforcement and the effective depth to the transverse
15.   reinforcement, in [mm];

16. f_c' the specified concrete compressive strength, in [MPa], and the limit of $\sqrt{f_c'}$ is 100 psi (8.3 MPa).

17. The punching shear capacity is compared to the shear stress on the critical perimeter. This critical perimeter is taken
18. at $d/2$ from the periphery of the loaded area, as was determined in seminal punching shear experiments (Moe, 1961).
19. The idea behind the ACI equations for punching shear is that the shear stress on the punching perimeter will be
20. limited, so that a ductile flexural failure will always occur before a brittle shear failure.
21.   For eccentric loading conditions, the shear stress on the critical perimeter is composed of the direct shear
22. v_{ug} and a contribution to the shear stress from the unbalanced moments, $\gamma_v M_{sc}$, see Figure 1. The total maximum
23. factored shear stress on the perimeter is then calculated as the largest absolute value of:

24.
$$v_{u,AB} = v_{ug} + \frac{\gamma_v M_{sc} c_{AB}}{J_c} \tag{11}$$

25.
$$v_{u,CD} = v_{ug} - \frac{\gamma_v M_{sc} c_{CD}}{J_c} \tag{12}$$

26. with
27. v_{ug} the factored shear stress determined at the centroidal axis of the critical section:

28.
$$v_{ug} = \frac{V_u}{b_o d} \tag{13}$$

29. V_u the factored shear force determined at the centroidal axis of the critical section;
30. γ_v a parameter that determines the fraction of moment transferred by eccentricity of shear:

31.
$$\gamma_v = 1 - \gamma_f \tag{14}$$

32.
$$\gamma_f = \frac{1}{1 + \left(\dfrac{2}{3}\right)\sqrt{\dfrac{b_1}{b_2}}} \tag{15}$$

33. b_1 dimension of the critical section b_o measured in the direction of the span for which moments are
34.   determined;

1   b_2 dimension of the critical section b_o measured in the direction perpendicular to b_1;
2   M_{sc} the factored slab moment that is resisted by the column at a joint;
3   J_c a property of the assumed critical section analogous to the polar moment of inertia. ACI 318-14 R8.4.4.2.3
4   gives an expression for an internal column, and mentions that similar equations can be developed for edge
5   and corner columns.
6 The distances c_{AB} and c_{CD} are as shown in Figure 1. Figure 1 also shows the combination of the shear contributions
7 of direct shear and unbalanced moment from Eqs. (14) and (15). This proposed simplified method is based on
8 experimental observations (Hanson and Hanson, 1968). However, revisiting these test results (Alexander and
9 Simmonds, 2003) showed that the contribution of unbalanced moments is lower than calculated with this method.
10

(a)   (b)
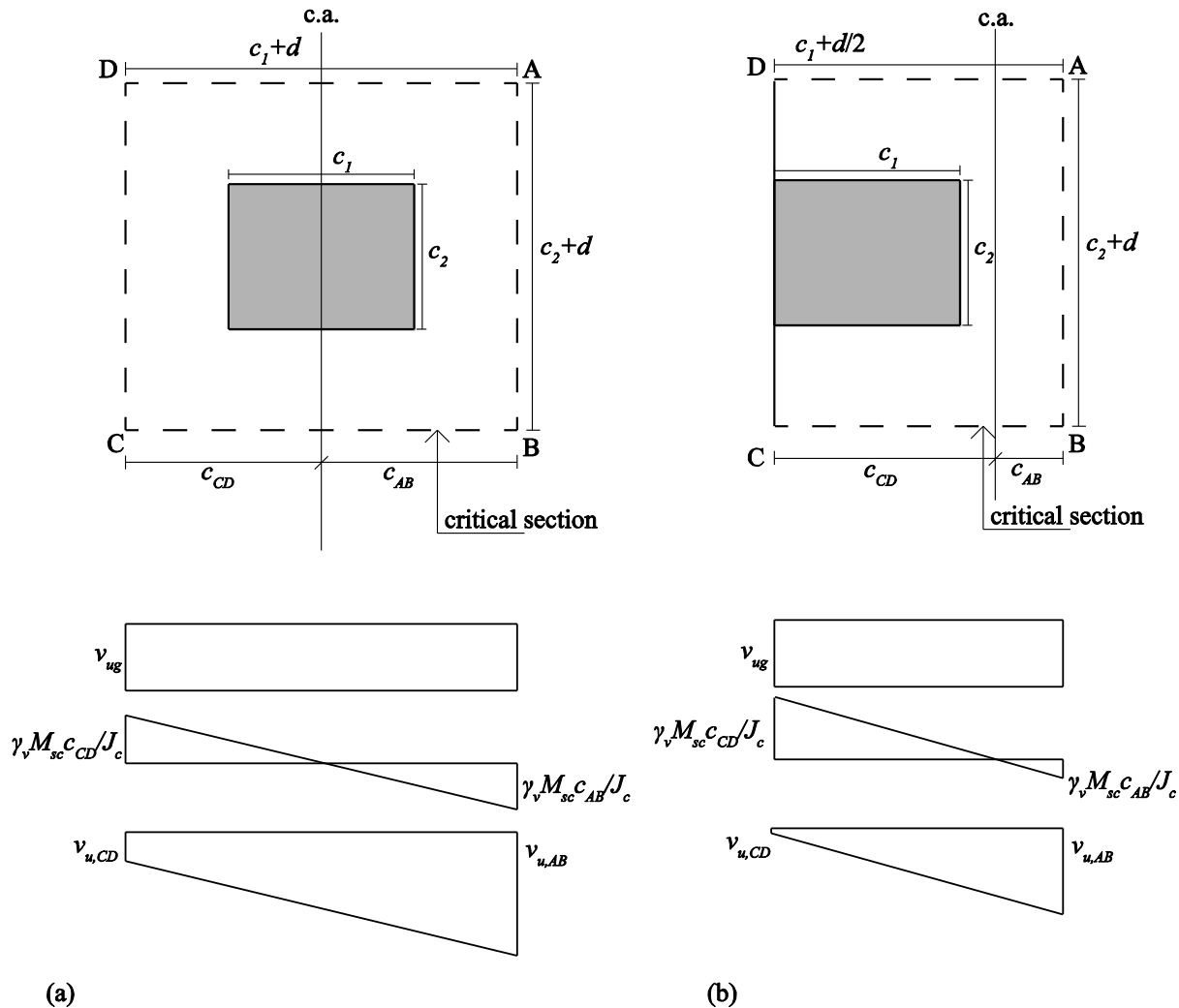
Figure 1 – Determination of governing factored shear stress from the combination of direct shear and unbalanced moments: (a) for an interior column; (b) for an edge column.

AVAILABLE EXPERIMENTS

Short description of slab shear experiments

16   The analysis is carried out based on the slab shear experiments from Delft University of Technology
18 (Lantsoght et al., 2013; Lantsoght et al., 2015). The slabs that are modeled are half-scale models of reinforced
19 concrete solid slab bridges tested in the Stevin II Laboratory. The slabs are 5 m × 2.5 m × 0.3 m (16.4 ft × 8.2 ft ×
20 1.0 ft) and are placed in a test setup as shown in Figure 2. The load is applied through a steel plate of 200 mm × 200
21 mm (7.87 in × 7.87 in) or 300 mm × 300 mm (11.81 in × 11.81 in). The position of the load can be altered along the
22 width and length of the slab. In the width direction, the load can be placed in the middle of the slab (position M as
23 shown in Figure 2) or at 438 mm (17.22 in) from the edge (position E as shown in Figure 2). In the length direction,

the load is either placed at a center-to-center distance to the support of a = 600 mm (23.62 in) or a = 400 mm (15.75 in). Slabs S1 – S14 are supported by an HEM 300 beam (with a width of 300 mm = 11.81 in), with a layer of plywood and felt on top (see Figure 2). Slabs S15 – S18 are supported by 3 elastomeric bearings across the width, with dimensions of 350 mm × 280 mm × 45 mm (13.78 in × 11.02 in × 1.77 in) and with a compression stiffness of 2361 kN/mm (13480 kip/in). To model the behavior of continuous slabs, prestressing bars are used close to support 2 (sup 2 in Figure 2) to restrain the rotation of the slab. As a result, a moment is created over support 2, resulting in the same situation as in a multiple-span bridge.

(a)   (b)
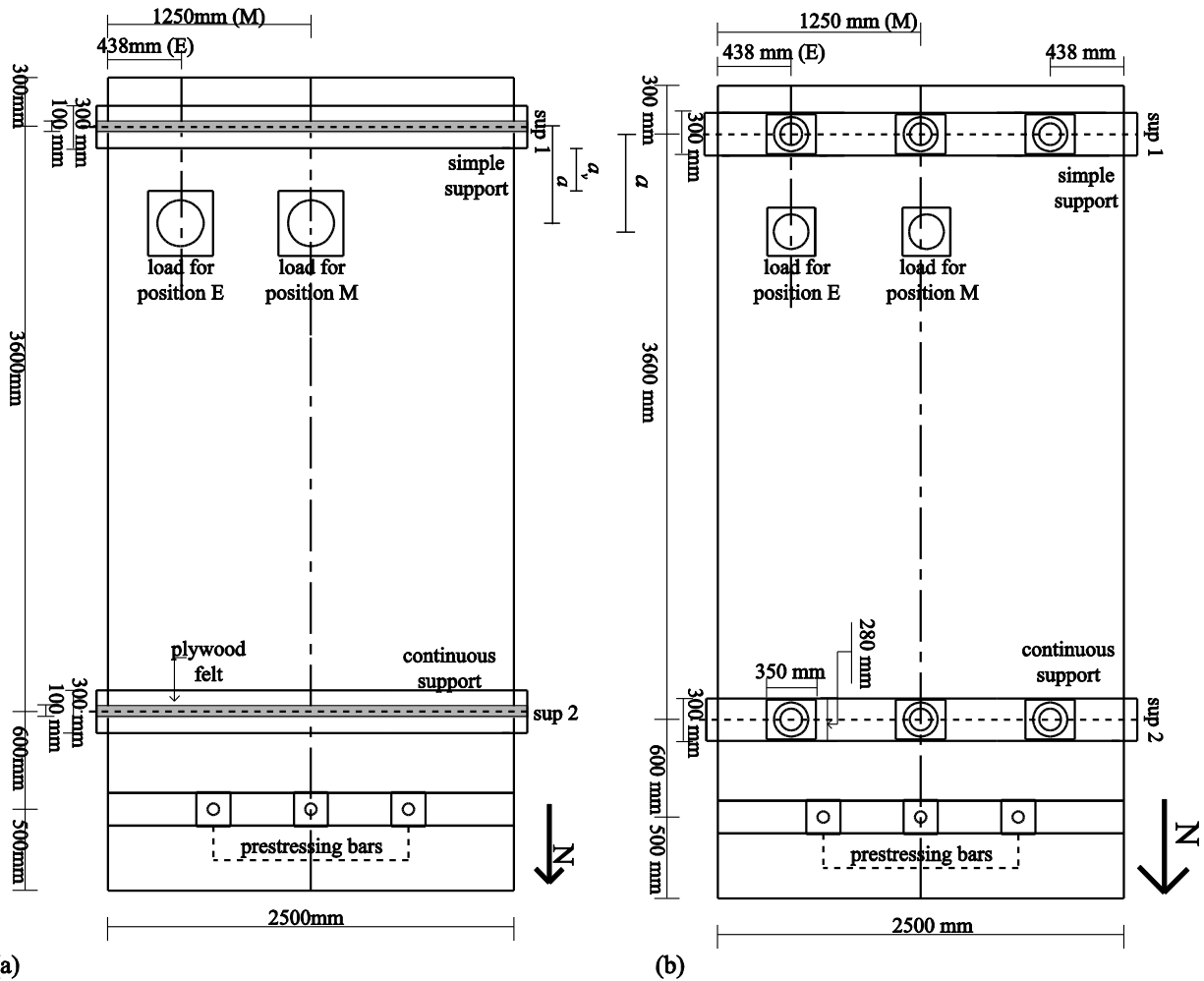
Figure 2 – Test setup for slab shear experiments: (a) with line supports; (b) supported by elastomeric bearings. Units: mm; 1 mm = 0.04 in.

In this paper, the main focus is on the slabs subjected to a single concentrated load placed close to the support (first series of experiments from the slab shear tests, S1 – S18), to evaluate how suitable the analyzed methods are for determining the shear capacity of asymmetrically loaded slabs. Slabs S1 to S18 from the slab shear experiments are analyzed here. An overview of the properties of these slabs is given in Table 1, using the following parameters:

$f_{c,cube}$	the measured mean cube compressive strength at the age of testing;
$f_{ct,meas}$	the mean measured splitting tensile strength tested on cubes at the age of testing;
ρ_l	the amount of longitudinal reinforcement;
ρ_t	the amount of transverse reinforcement;
a	the center-to-center distance between the load and the support;
d_l	the effective depth to the longitudinal reinforcement;
M/E	position of the load as shown in Figure 2;
z_{load}	the size of the side of the square loading plate used to transfer the load from the jack to the slab;

| 1 | Age | | | | | the age of the slab at the first test. | | |

1 Age   the age of the slab at the first test.

2   All slabs are 300 mm (11.81 in) thick. The effective depth to the longitudinal reinforcement, d_l, equals 265
3 mm (10.43 in) for slabs S1 – S14, and d_l = 255 mm (10.04 in) for S15 – S18. The effective depth to the transverse
4 reinforcement, d_t, equals 250 mm (9.84 in) for S1 – S14 and d_t = 232.5 mm (9.15 in) for S15 – S18. The resulting
5 reinforcement ratios are given in Table 1. Slabs S1-S10 and S15-S18 are reinforced with deformed bars of steel
6 S500. The measured capacities are f_{ym} = 542 MPa (78.61 ksi) for the mean yield strength and f_{um} = 658 MPa (95.44
7 ksi) for the mean ultimate strength for the 20 mm diameter bars (diameter of 0.79 in, closest to a #6 bar), and f_{ym} =
8 537 MPa (77.89 ksi); f_{um} = 628 MPa (91.08 ksi) for the 10 mm bars (diameter of 0.39 in, closest to a #3 bar). Slabs
9 S11-S14 are reinforced with plain bars with measured properties f_{ym} = 601 MPa (87.17 ksi) and f_{um} = 647 MPa
10 (93.84 ksi) for the 20 mm (0.79 in) diameter bars, and f_{ym} = 635 MPa (92.10 ksi) and f_{um} = 700 MPa (101.53 ksi) for
11 the 10 mm diameter bars. An overview of the results of the individual experiments is given in Table 2. Glacial river
12 aggregates with a maximum diameter of 16 mm (0.63 in) are used.

Table 1 – Overview of tested slabs. Conversion: 1 MPa = 145 psi, 1 mm = 0.04 in.

Slab nr.	$f_{c,cube}$ (MPa)	$f_{ct,meas}$ (MPa)	ρ_l (%)	ρ_t (%)	a/d_l	M/E	z_{load} (mm)	Age (days)
S1	35.8	3.1	0.996	0.132	2.26	M	200	28
S2	34.5	2.9	0.996	0.132	2.26	M	300	56
S3	51.6	4.1	0.996	0.258	2.26	M	300	63
S4	50.5	4.1	0.996	0.182	2.26	E	300	76
S5	46.2	3.6	0.996	0.258	1.51	M	300	31
S6	48.2	3.9	0.996	0.258	1.51	E	300	41
S7	82.1	6.2	0.996	0.258	2.26	E	300	83
S8	77.0	6.0	0.996	0.258	2.26	M	300	48
S9	81.7	5.8	0.996	0.258	1.51	M	200	77
S10	81.6	5.8	0.996	0.258	1.51	E	200	90
S11	54.9	4.2	1.375	0.358	2.26	M	200	90
S12	54.8	4.2	1.375	0.358	2.26	E	200	97
S13	51.9	4.2	1.375	0.358	1.51	M	200	91
S14	51.3	4.2	1.375	0.358	1.51	E	200	110
S15	52.2	4.2	1.035	1.078	2.35	M	200	71
S16	53.5	4.4	1.035	1.078	2.35	E	200	85
S17	49.4	3.7	1.035	1.078	1.57	M	200	69
S18	52.1	4.5	1.035	1.078	1.57	E	200	118

37 Comparison between slab shear experiments and code models
38   An overview of all experiments, and the calculated governing load effects and capacities, is given in Table 2.
39 In this table, the following parameters are given:
40 Test   name of the experiment, SxTy, with x the slab number (properties see Table 1) and y the number
41   of the test on this slab. Either two experiments were carried out (one at each support in position
42   M), or four (two at each support in position E);
43 b_r distance between the center of the load and the edge of the slab in the width direction;
44 SS/CS   experiment close to the simple support (SS) or continuous support (CS), see Figure 2;
45 P_u the maximum value of the concentrated load during the experiment;
46 Mode   the observed failure mode in the experiment:
47   WB: wide beam shear failure, indicated by inclined cracks on the bottom – the inclined crack is
48   not necessarily visible on the side face of the member;
49   P: punching shear failure;
50   B: beam shear failure with visible shear crack on the side face;
51   SF: failure by punching of the bearing of the support (for the slabs supported by discrete
52   elastomeric bearings);
53 F_{pres} the force in the prestressing bars;
54 V_{exp} the sectional shear force caused by the concentrated load, the self-weight of the slab, and the force
55   in the prestressing bars;

1	βV_{exp}	the sectional shear force caused by the concentrated load, the self-weight of the slab, and the force						
2		in the prestressing bars, for which the loads within $0.5d_l \leq a_v \leq 2d_l$ are reduced with the factor $\beta =$						
3		$a_v/2d_l$ according to the Eurocode shear provisions;						
4	V_{ACI}	the shear capacity according to the ACI 318-14 code;						
5	V_{Rc}	the shear capacity according to Eurocode 2;						
6	v_E	the governing shear stress on the punching perimeter according to Eurocode 2;						
7	v_u	the governing shear stress (from direct shear and unbalanced moment) on the punching perimeter						
8		according to ACI 318-14;						
9	v_{Rc}	the punching shear capacity according to Eurocode 2;						
10	v_c	the punching shear capacity according to ACI 318-14.						

11

12 **Table 2 – Overview of test results and calculated capacities: analysis with the shear and punching**
13 **provisions of Eurocode 2 and ACI 318-14. Conversion: 1 mm = 0.04 in; 1 kN = 0.225 kip; 1 MPa = 145 psi.**

Test	b_r (mm)	SS/CS	P_u (kN)	Mode	F_{pres} (kN)	V_{exp} (kN)	βV_{exp} (kN)	V_{ACI} (kN)	V_{Rc} (kN)	v_E (MPa)	v_u (MPa)	v_{Rc} (MPa)	v_c (MPa)
S1T1	1250	SS	954	WB	163	799	679	458	343	1.02	2.76	0.85	1.80
S1T2	1250	CS	1023	WB	138	912	784	458	343	1.10	3.09	0.85	1.80
S2T1	1250	SS	1374	WB + P	280	1129	848	450	384	1.44	3.25	0.95	1.77
S2T4	1250	CS	1421	WB	330	1276	985	450	384	1.49	3.57	0.95	1.77
S3T1	1250	SS	1371	WB	252	1131	851	550	439	1.43	3.25	1.21	2.17
S3T4	1250	CS	1337	WB + B	287	1199	925	550	439	1.40	3.36	1.21	2.17
S4T1	438	SS	1160	WB + B	203	964	727	494	333	1.92	2.91	1.14	2.17
S4T2	438	SS	1110	WB + B	187	925	698	494	333	1.83	2.79	1.14	2.17
S5T1	1250	CS	1804	WB + B	235	1679	681	338	329	2.85	4.67	2.37	2.09
S5T4	1250	SS	1755	WB + B	280	1544	573	338	329	2.77	4.36	2.37	2.09
S6T1	438	CS	1446	WB + B	183	1353	552	347	279	3.11	3.90	2.41	2.14
S6T2	438	CS	1423	WB + B	213	1337	550	347	279	3.06	3.85	2.41	2.14
S6T4	438	SS	1366	WB + B	195	1213	457	347	279	2.94	3.57	2.41	2.14
S6T5	438	SS	1347	WB + B	245	1187	442	347	279	2.90	3.51	2.41	2.14
S7T1	438	SS	1121	WB + P + B	217	929	700	623	389	1.85	2.81	1.41	2.73
S7T2	438	CS	1172	WB + P + B	197	1046	807	623	389	1.94	3.06	1.41	2.73
S7T3	438	CS	1136	WB + P + B	227	1021	789	623	389	1.88	2.98	1.41	2.73
S7T5	438	SS	1063	WB + P + B	157	891	673	623	389	1.76	2.68	1.41	2.73
S8T1	1250	SS	1481	WB + B	233	1226	923	672	502	1.55	3.52	1.38	2.65
S8T2	1250	CS	1356	WB + B	278	1213	936	672	502	1.42	3.40	1.38	2.65
S9T1	1250	SS	1523	WB + P	175	1355	640	440	331	2.49	4.62	2.26	2.73
S9T4	1250	CS	1842	WB + P	255	1717	851	440	331	3.02	5.77	2.26	2.73
S10T1	438	SS	1320	WB + P + B	162	1177	557	442	320	2.80	3.78	2.27	2.74
S10T2	438	SS	1116	WB + P + B	173	994	470	442	320	2.36	3.19	2.27	2.74
S10T4	438	CS	1511	WB + (B)	252	1422	712	442	320	3.20	4.46	2.27	2.74
S10T5	438	CS	1454	WB + B	235	1368	685	442	320	3.08	4.29	2.27	2.74
S11T1	1250	SS	1194	WB + P	165	998	848	567	441	1.28	3.45	1.23	2.23
S11T4	1250	CS	958	WB + P	307	886	766	567	441	1.03	2.97	1.23	2.23
S12T1	438	SS	931	WB + B + P	162	780	663	509	349	1.54	2.56	1.22	2.23
S12T2	438	SS	1004	P	173	839	712	509	349	1.66	2.76	1.22	2.23
S12T4	438	CS	773	WB + P + B	147	705	608	509	349	1.28	2.23	1.22	2.23
S12T5	438	CS	806	WB + B	158	735	633	509	349	1.33	2.32	1.22	2.23
S13T1	1250	SS	1404	WB + P	157	1253	593	351	317	2.30	4.26	2.16	2.17
S13T4	1250	CS	1501	WB + P	240	1411	706	351	317	2.46	4.73	2.16	2.17
S14T1	438	SS	1214	WB + P + B	133	1088	518	349	305	2.57	3.48	2.16	2.16
S14T2	438	SS	1093	WB + P + B	162	975	462	349	305	2.32	3.13	2.16	2.16
S14T4	438	CS	1282	WB + P + B	187	1207	605	349	305	2.72	3.79	2.16	2.16
S14T5	438	CS	1234	WB + P + B	142	1157	578	349	305	2.61	3.64	2.16	2.16
S15T1	1250	CS	1040	WB + B + SF	245	944	685	445	337	1.37	3.39	1.67	2.18

S15T4	1250	SS	1127	WB + SF	158	944	670	445	337	1.49	3.47	1.67	2.18
S16T1	438	SS	932	WB + B	188	776	551	440	283	1.78	2.69	1.69	2.21
S16T2	438	SS	815	WB + B	208	675	479	440	283	1.56	2.34	1.69	2.21
S16T4	438	CS	776	WB + B + SF	235	723	528	440	283	1.48	2.38	1.69	2.21
S16T5	438	CS	700	WB + B + SF	198	653	478	440	283	1.34	2.15	1.69	2.21
S17T1	1250	CS	1365	WB + SF	208	1285	449	252	261	3.05	4.58	3.77	2.18
S17T4	1250	SS	1235	WB + SF	118	1109	357	252	261	2.76	4.01	3.77	2.18
S18T1	438	SS	1157	WB + B + SF	170	1031	328	251	260	2.91	3.48	3.76	2.18
S18T2	438	SS	1079	WB + B	213	954	300	251	260	2.71	3.23	3.76	2.18
S18T4	438	CS	1122	WB + B + SF	167	1062	375	251	260	2.82	3.49	3.76	2.18
S18T5	438	CS	1104	WB + B + SF	190	1050	373	251	260	2.77	3.44	3.76	2.18

Discussion of results of symmetrical and asymmetrical loading

An overview of the results of the comparison between asymmetrically loaded slabs and the shear and punching provisions is given in Figure 3. The 45° line indicates the values for which the predicted and tested sectional shear forces or shear stresses are identical. Marks above this line indicate conservative predictions, while marks below this line indicate that the code provision overestimates the capacity of the element. From Figure 3, it can be seen that, in general, the code provisions are conservative. The lowest total average can be observed for the punching provisions of Eurocode 2. However, in a typical analysis, it would be found that the shear capacity is critical, and that shear failure would occur before punching failure. Compared to the experiments, the ACI provisions for shear and punching lead to a large scatter, whereas the results from Eurocode 2 show less scatter. In general, the results also show that extrapolating the shear and punching provisions from the codes to the application of slab bridges subjected to concentrated wheel loads results in larger scatter than when analyzing slab-column connections or beam shear tests in four point bending. The code equations are thus less suitable for asymmetrical loading situations.

The statistical analysis (with AVG = average, STD = standard deviation, and COV = coefficient of variation) is given in Table 3. In this Table, the following subsets of data are analysed:
- S1-S18: all experiments of slabs subjected to a single concentrated load close to the support;
- M: all experiments for which the concentrated load is placed in the middle of the width;
- E: all experiments for which the concentrated load is placed close to the edge;
- S1-S6: all experiments on normal strength concrete slabs supported by line supports ;
- S7-S10: all experiments on high strength concrete slabs;
- S11-S14: all experiments on slabs with plain reinforcement bars:
- S15-S18: all experiments on slabs supported by elastomeric bearings.

From the results in Table 3, it can be seen that both ACI 318-14 and Eurocode 2 indicate that these slabs would fail in beam shear before punching shear. Comparing the average values for loading situation "M" and loading situation "E" also shows that all methods (except the Eurocode punching provisions) give less conservative values as the loading situation becomes more asymmetric. The coefficient of variation on the shear prediction of ACI 318-14 is very large, and indicates that the shear provisions from ACI 318-14 are not very suitable for extrapolation to the shear capacity of slabs under concentrated loads. However, Figure 3a indicates that ACI 318-14 gives conservative estimates for all experiments. The results of the comparison between the tested and predicted values with ACI 318-14 shows that the average tested-to-predicted value is lower for slabs of high strength concrete than for slabs of normal strength concrete, for slabs with plain reinforcement bars as compared to slabs with ribbed reinforcement bars, and for slabs supported by line supports as compared to slabs supported by discrete elastomeric bearings.

Of the analysed methods, the Eurocode one-way shear predictions give the lowest coefficient of variation. Again, the average tested-to-predicted value is lower for the slabs of high strength concrete than for slabs with normal strength concrete, and for slabs with plain reinforcement bars as compared to slabs with deformed reinforcement bars. The tested-to-predicted value for slabs supported by elastomeric bearings is also smaller than for slabs on line supports, because of the load reduction factor β.

The punching shear capacity from ACI 318-14, with the governing shear stress on the punching perimeter caused by direct shear and unbalanced moment, has a lower coefficient of variation for slabs under concentrated loads close to supports than the one-way shear capacity. Again, the tested-to-predicted values for normal strength concrete are higher than for high strength concrete, and lower for plain reinforcement bars as compared to deformed

bars. The tested-to-predicted values for the punching capacity are lower on average for slabs supported by bearings than for slabs on line supports.
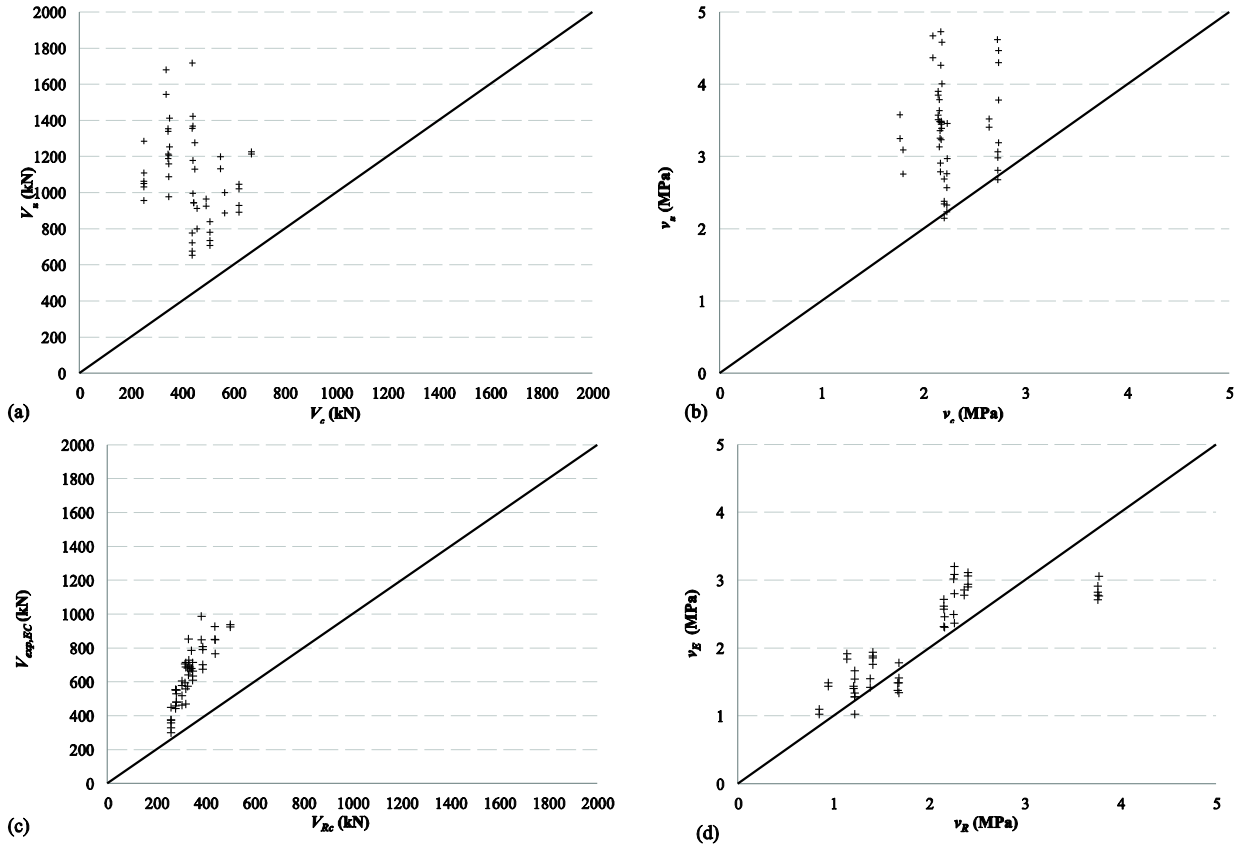
Figure 3 – Comparison between experiments on asymmetrically loaded slabs and code provisions: (a) ACI 318-14 shear provisions; (b) ACI 318-14 punching provisions; (c) Eurocode 2 shear provisions; (d) Eurocode 2 punching provisions. Conversion: 1 kN = 0.225 kip; 1 MPa = 145 psi.

For the Eurocode 2 results, the coefficient of variation is larger on the tested-to-predicted results for punching than for shear. The average value of the tested-to-predicted ratio is closer to 1, indicating a closer prediction of the experimental results. However, using Eurocode 2 would have indicated shear failure before punching failure. The tested-to-predicted ratios with the Eurocode 2 formula have a similar average for loading situation "M" and "E", indicating that the way Eurocode 2 takes varying degrees of asymmetry into account for punching is better than the other shear and punching models under consideration. Again, the tested-to-predicted value is higher on average for the slabs with normal strength concrete as compared to slabs with high strength concrete. The average tested-to-predicted ratio is lower for the slabs reinforced with plain bars as compared to slabs with deformed bars. For the slabs supported by elastomeric bearings, the Eurocode 2 provisions for punching of the load are unconservative. However, it must be noted that an assessment based on Eurocode 2 would have predicted shear failure before punching failure, and that in the experiments punching of the elastomeric bearings were observed as a secondary failure mode.

The results from Table 3 can be compared to values from the literature. For the ACI 318-14 formula, originally recommended in 1962 (ACI-ASCE Committee 326, 1962), the tested-to-predicted value was 1.076 with a coefficient of variation of 15.8%. For this analysis, the results of 194 beams failing in shear were used. Later, it was shown that this formula becomes unsafe when extrapolated to deep members and lightly reinforced members (Collins et al., 2008).

For the Eurcode 2 shear formula (previously used in the Model Code 1990 (CEB-FIP, 1993)), an average tested-to-predicted value of 0.92 with a standard deviation of 0.12 and a coefficient of variation of 13% was found (König and Fischer, 1995). For this comparison, a database of experiments on beams failing in shear was used.

The Eurocode 2 punching expression resulted in a mean tested-to-predicted ratio of 1.01 with a standard deviation of 0.14 and a coefficient of variation of 14%, whereas the ACI 318-14 expression resulted in a mean of 1.54, a standard deviation of 0.32 and a coefficient of variation of 21% (Gardner, 2011). The experiments for both these comparisons are taken from the *fib* punching database (fib Task Group on Utilisation of concrete tension in design, 2001).

Table 3 – Statistical analysis of comparison between experimental results, and shear and punching provisions from ACI 318-14 and Eurocode 2.

		S1-S18	M	E	S1-S6	S7-S10	S11-S14	S15-S18
V_{exp}/V_{ACI}	AVG	2.71	2.91	2.58	2.95	2.34	2.47	3.04
	STD	1.09	1.19	1.02	1.08	0.82	1.00	1.36
	COV (%)	40.3	41.0	39.5	36.4	35.2	40.4	44.8
$\beta V_{exp}/V_{Rc}$	AVG	1.87	2.00	1.79	2.02	1.95	1.86	1.63
	STD	0.29	0.28	0.27	0.26	0.28	0.18	0.30
	COV (%)	15.6	14.2	15.2	12.8	14.5	9.8	18.2
v_u/v_c	AVG	1.52	1.75	1.37	1.71	1.37	1.50	1.47
	STD	0.34	0.30	0.28	0.27	0.33	0.37	0.33
	COV (%)	22.5	17.3	20.4	15.9	24.5	24.4	22.6
v_E/v_{Rc}	AVG	1.14	1.11	1.16	1.33	1.24	1.13	0.82
	STD	0.24	0.22	0.25	0.18	0.14	0.14	0.10
	COV (%)	20.8	20.1	21.4	13.7	10.9	12.1	12.0
P_{exp}/P_{ESM}	AVG	1.61	1.64	1.58	1.67	1.59	1.59	1.56
	STD	0.21	0.23	0.20	0.20	0.20	0.20	0.26S
	COV (%)	13.3	14.0	12.8	11.9	12.4	12.7	16.6

The results in Table 3 show that the ACI 318-14 shear expression underestimates the capacity of slabs under concentrated loads close to supports more than beams, but also has a much larger coefficient of variation. As such, it can be concluded that the formula gives a (very) conservative estimate of the shear capacity of slabs under concentrated loads close to supports, but might not be suitable for extrapolation to this loading case. For the shear formula from Eurocode 2, the coefficient of variation of the slab shear and beam shear experiments is comparable. The large difference is in the average tested-to-predicted value, which turns out to be much larger for slabs than for beams. This observation can be explained by the ability of slabs to activate transverse distribution (Lantsoght et al., in press), resulting in larger shear capacities than beams. The results of the ACI 318-14 punching shear equation is similar when compared to the *fib* punching database as well as when compared to the slab shear experiments. This observation might indicate that the simple method from Figure 1 for asymmetrically loaded slabs leads to an acceptable estimate of the punching shear capacity. However, it must be noted that the coefficient of variation of the tested-to-predicted ratio in Table 3 is still rather large. Finally, comparing the results of the analysis of the *fib* punching database with regard to the performance of the Eurocode 2 punching formula to the results of the analysis of the slab shear experiments shows that the average tested-to-predicted values are of a similar magnitude. However, the coefficient of variation becomes larger for the slab shear experiments, indicating that not all parameters considered in the experiments are reflected by the Eurocode 2 punching equation in a correct manner.

Similar observations were made when comparing different finite element models. For loading cases with loads at an asymmetric position with respect to both axis of symmetry of the slab, the prediction with the finite element model was farther away from the experimental result than for the case with a load at an asymmetric position with respect to only one axis of symmetry of the slab (Lantsoght et al., 2016b).

EXTENDED STRIP MODEL

Description of model

The Extended Strip Model is the application to slabs under concentrated loads close to supports (asymmetrically loaded slabs) of the Bond Model or Strip Model for concentric punching shear (Alexander and Simmonds, 1992). With the Strip Model, a slab-column connection is subdivided into quadrants and strips, see Figure 4. The strips work in arching action, whereas the quadrants work in two-way flexure. The governing stress is the stress at the interface between the strips and the quadrants, which can be quantified as the one-way shear stress. The maximum load at the slab-column connection is then found by summing the contributions of the four radial strips.

1   Applying the Strip Model to asymmetric loading cases such as a concentrated load on a slab requires a few
2 extensions to the model. First of all, because of the positions of the load and supports (a situation as shown for
3 example in Figure 2), the sectional shear force will not be identical at both faces of the loaded area. Therefore, one
4 side will reach the limiting shear stress on the interfaces while the other side will be subjected to a lower shear
5 stress. Failure then will not occur at all four strip interfaces at the same time, but instead just at the strip interfaces
6 subjected to the largest shear stresses.
7
8
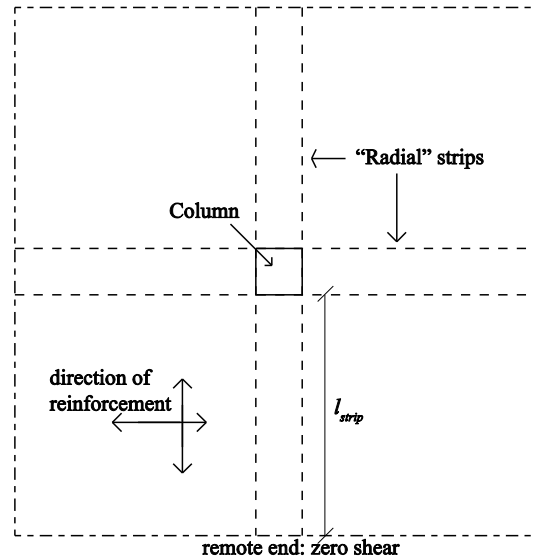
9
10 **Figure 4 – Layout of quadrants and strips (Alexander and Simmonds, 1992).**
11
12   The Extended Strip Model takes into account the increase in capacity caused by the compression strut (or
13 arch) that occurs between the applied load and the support for loads close to the support. The capacity of the strip
14 between the load and the support can be enhanced, and the factor used for this magnification is as determined by
15 Regan for parts of a punching perimeter close to supports (Regan, 1982). Additionally, the effect of torsion needs to
16 be taken into account (Valdivieso et al., 2016).
17   For concentrated loads on continuous slabs, the reinforcement resisting the tension caused by the hogging
18 moment will be activated in the region between the load and the support. Therefore, the capacity of the strips in this
19 region will be increased. The capacity will not be determined purely by the sum of the sagging moment and hogging
20 moment capacities, but instead is governed by the sum of the sagging moment capacity and a fraction of the hogging
21 moment capacity. This fraction is taken as the ratio of the support moment to the span moment for the considered
22 loading case (Lantsoght et al., (in review)).
23   The effect of torsion on asymmetrically loaded slabs becomes considerable as the asymmetry increases. For
24 the slab shear experiments (Figure 2), the loading situation "E" is asymmetric in both the length and width direction,
25 and the loading situation "M" only in the length direction. The relative effect of the torsional moments will thus be
26 larger for loading situation "E". When the torsional moments become larger, the capacity of the strip-quadrant
27 interfaces will be smaller as a result of shear-torsion interaction. Therefore, a reduction factor was built into the
28 model, which reduces the capacity of the strips when the torsional moment is relative larger with respect to the
29 bending moment. This study was based on a sensitivity study with linear finite element models (Valdivieso et al.,
30 2016).
31   Another effect that occurs for loads placed close to the slab edge, is that the length of the strip geometrically
32 available can be smaller than the loaded strip length used for finding the most unfavorable loading situation on the
33 strip. For these cases, the loaded strip length must be limited to the actual maximum strip length available. This
34 reduction is the application of the so-called "edge effect" (Lantsoght et al., (in review)).
35   For slabs supported by bearings, the increase in capacity for loads placed close to the support is less, as the
36 reduced support length allows for less anchorage of the strut. For slabs reinforced with plain bars, the reduction of
37 the bond between the steel and the concrete will lead to a slightly smaller shear capacity for the interface between
38 the strips and the quadrants. A factor 0.7 was proposed for this effect. This factor was determined empirically to take
39 into account the lower bond between the concrete and the plain reinforcement bars, reducing the shear capacity at

the interface between the strips and quadrants. A correction for the size effect was also added to the model, and the effect of self-weight can be subtracted from the shear stress at the interface between the quadrants and strips, for the interfaces in the span direction (Lantsoght, 2016). A full description of the model, as well as a step-by-step explanation of the procedure, is given elsewhere (Lantsoght et al., (in review)). The method can also be applied for the assessment of existing slab bridges (Lantsoght et al., 2016a). The resulting equations for the Extended Strip Model are:

$$P_x = \sqrt{2(1+\beta_t)M_{sag,x}w_{ACI,x}} \tag{16}$$

$$P_{sup} = \frac{2d_x}{a_v}\sqrt{2(1+\beta_t)M_{s,x}w_{ACI,x}} \tag{17}$$

$$P_{sup} = \sqrt{2(1+\beta_t)M_{s,x}w_{ACI,x}}\beta_{sup} \tag{18}$$

$$P_y = \sqrt{2\left(\frac{L}{L-a_M}\right)M_{s,y}\left(w_{ACI,y}-v_{DL}\right)} \tag{19}$$

$$P_{edge} = \begin{cases} \sqrt{2\beta_t\left(\frac{L}{L-a_M}\right)M_{s,y}\left(w_{ACI,y}-v_{DL}\right)} \text{ for } l_w < l_{edge} \\ \beta_t\left(\frac{L}{L-a_M}\right)\left(w_{ACI,y}-v_{DL}\right)l_{edge} \text{ for } l_w \geq l_{edge} \end{cases} \tag{20}$$

with

P_x the capacity of a strip in the longitudinal direction, in [N];

P_{sup} the capacity of a strip between the load and the support in the longitudinal direction, in [N], with Eq. (17) for slabs supported by line supports and Eq. 18 for slabs on discrete bearings;

P_y the capacity of a strip in the transverse direction, in [N];

P_{edge} the capacity of a strip between the load and the free edge in the transverse direction, in [N];

β_t factor for the effect of torsion, derived from linear finite element models (unitless) (Valdivieso et al., 2016):

$$\beta_t = 0.8\frac{a}{d_l}\frac{b_r}{b} \text{ for } 0 \leq \frac{a}{d_l} \leq 2.5 \text{ and } 0 \leq \frac{b_r}{b} \leq \frac{1}{2} \tag{21}$$

a the center-to-center distance between the load and the support, in [mm];

d_l the effective depth to the longitudinal reinforcement, in [mm];

b_r the distance between the center of the load and the free edge, in [mm];

b the width of the slab, in [mm];

$M_{sag,x}$ the sagging moment capacity of the longitudinal reinforcement, in [Nmm]:

$$M_{sag,x} = \rho_{sag,x}f_{yk}bd_l^2\left(1-\frac{f_{yk}\rho_{sag,x}}{1.7f_{ck}}\right) \tag{22}$$

$M_{hog,x}$ the hogging moment capacity of the longitudinal reinforcement, in [Nmm]:

$$M_{hog,x} = \rho_{hog,x}f_{yk}b\left(d_l'\right)^2\left(1-\frac{f_{yk}\rho_{hog,x}}{1.7f_{ck}}\right) \tag{23}$$

$M_{sag,y}$ the sagging moment capacity of the transverse reinforcement, in [Nmm]:

$$M_{sag,y} = \rho_{sag,y}f_{yk}l_{span}d_t^2\left(1-\frac{f_{yk}\rho_{sag,y}}{1.7f_{ck}}\right) \tag{24}$$

$M_{hog,y}$ the hogging moment capacity of the transverse reinforcement, in [Nmm]:

$$M_{hog,y} = \rho_{hog,y}f_{yk}l_{span}\left(d_t'\right)^2\left(1-\frac{f_{yk}\rho_{hog,y}}{1.7f_{ck}}\right) \tag{25}$$

$M_{s,x}$ the bending moment capacity of the longitudinal reinforcement, in [Nmm]:

$$M_{s,x} = M_{sag,x} + \lambda_{moment}M_{hog,x} \tag{26}$$

| 1 | $M_{s,x}$ | the bending moment capacity of the transverse reinforcement, in [Nmm]: | |
| 2 | | $$M_{s,y} = M_{sag,y} + \lambda_{moment} M_{hog,y}$$ | (27) |

1 $M_{s,x}$ the bending moment capacity of the transverse reinforcement, in [Nmm]:

$$M_{s,y} = M_{sag,y} + \lambda_{moment} M_{hog,y} \tag{27}$$

3 $\rho_{sag,x}$ the reinforcement ratio of the longitudinal sagging moment reinforcement (unitless);

4 $\rho_{hog,x}$ the reinforcement ratio of the longitudinal hogging moment reinforcement (unitless);

5 $\rho_{sag,y}$ the reinforcement ratio of the transverse sagging moment reinforcement (unitless);

6 $\rho_{hog,y}$ the reinforcement ratio of the transverse hogging moment reinforcement (unitless);

7 d_l' the effective depth to the longitudinal hogging moment reinforcement, in [mm];

8 d_t the effective depth to the transverse sagging moment reinforcement, in [mm];

9 d_t' the effective depth to the transverse hogging moment reinforcement, in [mm];

10 l_{span} the span length, in [mm];

11 f_{yk} the characteristic yield strength of the steel, in [MPa];

12 f_{ck} the characteristic concrete compressive strength, in [MPa];

13 λ_{moment} the ratio of support moment to span moment under the considered loading case, $\lambda_{moment} = M_{sup}/M_{span}$

14 (unitless);

15 $w_{ACI,x}$ the shear capacity of the interface between the quadrant and strip in the x-direction, taking the size effect

16 into account, in [N/mm = kN/m]:

$$w_{ACI,x} = 0.166 d_t \sqrt{f_{ck}} \left(\frac{100mm}{d}\right)^{\frac{1}{3}} \tag{28}$$

18 $w_{ACI,y}$ the shear capacity of the interface between the quadrant and strip in the y-direction, in [N/mm = kN/m]:

$$w_{ACI,y} = 0.166 d_l \sqrt{f_{ck}} \left(\frac{100mm}{d}\right)^{\frac{1}{3}} \tag{29}$$

20 d the average of the effective depth in the longitudinal and transverse direction, in [mm];

21 β_{sup} the factor for loads close to supports when discrete supports are used (unitless):

$$\beta_{sup} = 1 \text{ for } 1.5 \le \frac{a_v}{d_l} \le 2$$

22 $$\beta_{sup} = 1.6 - 0.4 \frac{a_v}{d_l} \text{ for } 0.5 \le \frac{a_v}{d_l} \le 1.5 \tag{30}$$

$$\beta_{sup} = 1.4 \text{ for } \frac{a_v}{d_l} < 0.5$$

23 L the length between points of contraflexure, in [mm];

24 a_M the distance between the load and the support or between the load and the point of contraflexure, whichever

25 is nearer, in [mm];

26 v_{DL} shear force on the interface between the load and the support caused by the self-weight of the slab, in

27 [N/mm];

28 l_{edge} the distance between the free edge and the face of the load, in [mm];

29 l_w the loaded length of the strip, in [mm]:

$$l_w = \sqrt{\frac{2M_{s,y}}{\beta_t \left(w_{ACI,y} - v_{DL}\right) \frac{L}{L - a_M}}} \tag{31}$$

31

32 Comparison between Extended Strip Model and asymmetrically loaded slabs

33   The slab shear experiments are compared to the Extended Strip Model. The maximum load in the experiment

34 is shown as P_{exp} and the maximum concentrated loads as calculated with the Extended Strip Model is given as P_{ESM}.

35 The statistical parameters are given in Table 3. The first conclusion that can be drawn from the results in Table 3 is

36 that the Extended Strip Model gives a better prediction of the experiments than the code provisions, as the lowest

37 coefficient of variation is obtained. Comparing the results from the column with loading cases "M" and "E" shows

38 that the difference is rather small. The tested-to-predicted ratio is slightly smaller for the loading case "E", but the

39 difference between loading cases "M" and "E" is almost negligible. For the reference subset, slabs S1-S6, the

40 Extended Strip Model results in the lowest coefficient of variation.

41   For the high strength concrete slabs, the tested-to-predicted ratio is only marginally smaller, indicating that

42 the model reflects the influence of the concrete compressive strength correctly. For the slabs reinforced with plain

1   bars, $w_{ACI,x}$ from Eq. (28) and $w_{ACI,y}$ from Eq. (29) the shear strength needs to be multiplied with a factor 0.7. This
2   factor was determined empirically to take into account the lower bond between the concrete and the plain
3   reinforcement bars, reducing the shear capacity at the interface between the strips and quadrants. The results in
4   Table 3 indicate that this choice leads to good results.
5   For the slabs supported by elastomeric bearings, the increase in capacity of the strip between the load and the
6   support needs to be calculated with β_{sup} from Eq. (30). The statistical parameters of the tested-to-predicted results for
7   S15-S18 show that this subset results in the largest coefficient of variation. An element of empiricism in the
8   Extended Strip Model when applied to slabs on discrete bearings is the use of β_{sup}.
9   A graphical overview of the comparison between the Extended Strip Model and the test results, as well as the
10 histogram of the tested-to-predicted ratios, is given in Figure 5. The results from this histogram show that the 5%
11 lower bound is larger than 1, so that the method is suitable for design, and the results from Figure 5a show that the
12 trend of the tested-to-predicted ratios is parallel with the 45^0 line. This observation indicates that the range of
13 parameters that is studied in the experiments is represented well by the model, an observation that could not be made
14 for the code provisions, shown in Figure 2, except perhaps for the Eurocode punching provisions.
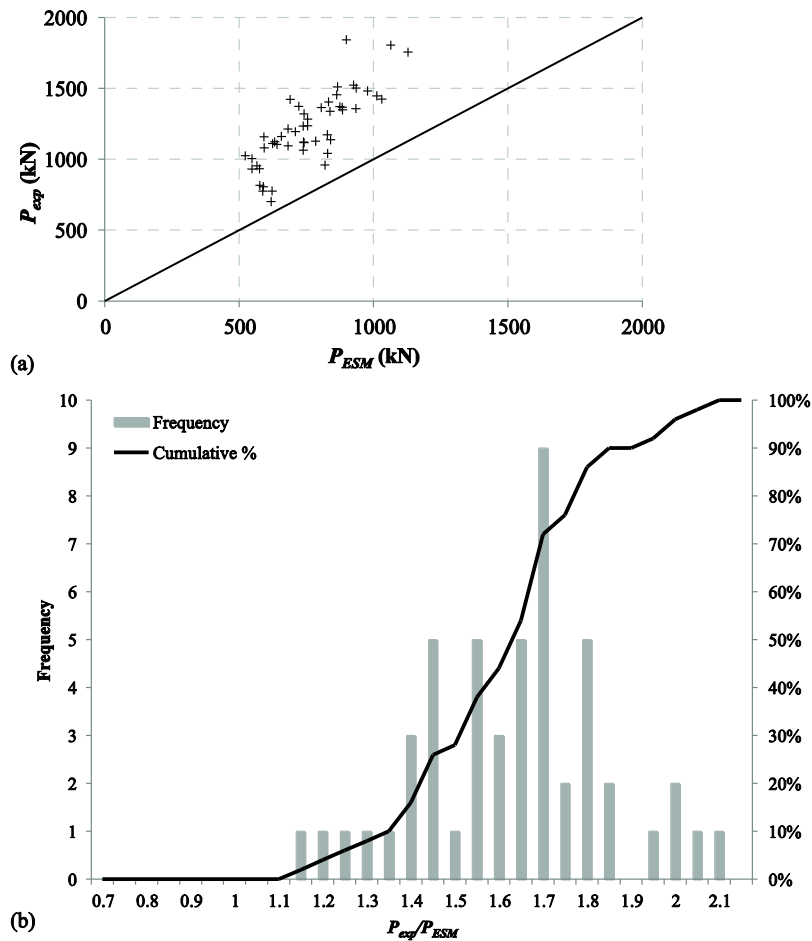15

(a)

(b)

16
17 **Figure 5 -- Comparison between slab shear experiments and Extended Strip Model: (a) overview; (b)**
18 **histogram. Conversion: 1 kN = 0.225 kip.**
19

20   DISCUSSION
21   Whereas most beam shear and punching shear provisions from the governing codes were developed for
22 symmetric loading cases, and lead to increasing levels of inaccuracy for loading cases that are more and more
23 asymmetric, the (Extended) Strip Model performs equally well for symmetric and asymmetric loading cases. The
24 original Strip Model (or Bond Model) for concentric punching shear was developed for a symmetric loading case.
25 With a few modifications and extensions to the model to make it applicable to asymmetric loading cases, it was

shown that the Extended Strip Model leads to satisfactory results when compared to experimental results of slabs failing in shear.

One of the strengths of the Extended Strip Model is that it combines two-way flexure, beam shear, and punching shear. For typical bridge deck slabs subjected to concentrated wheel loads, the failure mechanism tends to be a combination of flexure, beam shear, and punching shear. The model is thus suitable to study such complex loading cases.

The Extended Strip Model currently has a few elements of empiricism:

- the shear capacity of the interface between the quadrants and strips (Eqs. (28) and (29)) uses the limiting shear strength from ACI 318-14;
- the size effect factor on the shear capacity of the interface between the quadrants and strips is empirical;
- the reduction (using a factor of 0.7) of the shear capacity of the interface between the quadrants and strips for slabs reinforced with plain bars is empirical;
- the factor β_{sup} for slabs supported by discrete bearings is determined empirically.

The limiting shear strength from ACI 318-14 also includes the upper limit to $\sqrt{f_c{'}}$ of 100 psi (8.3 MPa), until further experimental evidence can be used to investigate the need for this upper limit. Another limitation of the Extended Strip Model is that it requires yielding of the reinforcement at the ultimate limit state. For slabs with heavy flexural reinforcement in which a shear failure occurs before yielding of the steel, the model cannot be used. Practical cases of slabs do not have this type of reinforcement, but sometimes slabs tested in laboratories are heavily reinforced to make sure the slab fails in punching or shear before it fails in flexure.

SUMMARY AND CONCLUSIONS

Reinforced concrete slabs are subjected to asymmetric loading cases when unbalanced moments occur in buildings at the slab-column connection, and in bridges subjected to concentrated live loads. The majority of the existing code equations were derived either based on experiments on symmetric loading cases, or were derived as mechanical models, but then compared and fitted to experiments on symmetric loading cases. Asymmetrically loaded slabs tested in laboratories are limited to slab-column connections with an unbalanced moment, not extending past the point of contraflexure.

In this paper, asymmetrically loaded slabs are studied. Experiments on slabs under a single concentrated load applied close to the support are used for the analysis. The experimental results are compared to the capacities as predicted by Eurocode 2 and ACI 318-14. Both codes would conservatively predict a one-way shear failure to occur before two-way shear failure in the tested slabs. The overall best prediction is delivered by the one-way shear provisions from Eurocode 2, which gives the lowest coefficient of variation. The large average value of the tested-to-predicted ratio however indicates the large conservativism of the method. In general, the coefficients of variation of the tested-to-predicted ratios when comparing the slab shear experiments to the predicted values from Eurocode 2 and ACI 318-14 are larger than when the punching provisions are compared to slab-column connection tests, or when the beam shear provisions are compared to beam shear tests, as reported in the literature.

The Extended Strip Model, an extension of the Strip Model or Bond Model for concentric punching shear, is suitable to determine the maximum load on asymmetrically loaded reinforced concrete slabs. The model combines two-way flexure, one-way shear, and two-way shear, and as such, the model is suitable for more complex loading cases, e.g. slab bridges subjected to concentrated wheel loads, which fail in a combination of flexure, one-way shear, and two-way shear. For asymmetric loading cases, the effect of torsion, which reduces the capacity, needs to be taken into account. For loads close to the free edge, the edge effect needs to be considered, i.e. it needs to be studied if the entire loaded length of the strip between the load and the free edge can develop. The effect of different reinforcement ratios in the longitudinal and transverse direction should be considered, as well as the shear and moment diagrams occurring for the asymmetric loading situation. The model is also extended with empirically determined parameters for slabs reinforced with plain bars and slabs supported by discrete bearings.

When the Extended Strip Model is compared with the experimental results from slabs subjected to symmetrical loading conditions, it is found that the model leads to a good and conservative prediction of the maximum load that can be applied to a slab. The coefficient of variation of the tested-to-predicted results is lower than with any of the studied code methods, and the model gives consistent statistical parameters across different subsets of the experimental data. It can thus be concluded that the Extended Strip Model, which is simple enough for hand calculations, gives a good prediction of the capacity of asymmetrically loaded reinforced concrete slabs, when a concentrated load is used.

REFERENCES

AASHTO, 2015, "AASHTO LRFD bridge design specifications, 7th edition with 2015 interim specifications," 7th ed. American Association of State Highway and Transportation Officials; Washington, DC.

ACI-ASCE Committee 326, 1962, "Shear and Diagonal Tension: Part 2 - Beams and Frames," *Journal of the American Concrete Institute*, V. 59, No. 2, pp. 277-333.

ACI Committee 318, 2014, "Building code requirements for structural concrete (ACI 318-14) and commentary," American Concrete Institute; Farmington Hills, MI, 503 pp.

Adebar, P. and Collins, M. P., 1996, "Shear strength of members without transverse reinforcement," *Canadian journal of civil engineering*, V. 23, No. 1, pp. 30-41.

Alexander, S. D. B. and Simmonds, S. H., 1987, "Ultimate Strength of Slab-Column connections," *ACI Structural Journal*, V. 84, No. 3, pp. 255-261.

Alexander, S. D. B. and Simmonds, S. H., 1992, "Bond Model for Concentric Punching Shear," *ACI Structural Journal*, V. 89, No. 3, pp. 325-334.

Alexander, S. D. B. and Simmonds, S. H., 2003, "Moment transfer at interior slab-column connections," *ACI Structural Journal*, V. 100, No. 2, Mar-Apr, pp. 197-202.

ASCE-ACI Task Committee 426, 1974, "Shear-Strength of Reinforced-Concrete Members - Slabs," *Journal of the Structural Division-ASCE*, V. 100, No. NST8, pp. 1543-1591.

Barzegar, F., Echle, R. and Foroozesh, M., 1991, "Moment Transfer and Slab Effective Widths in Laterally Loaded Edge Connections," *ACI Structural Journal*, V. 88, No. 5, Sep-Oct, pp. 615-623.

Belletti, B., Pimentel, M., Scolari, M. and Walraven, J. C., 2015, "Safety assessment of punching shear failure according to the level of approximation approach," *Structural Concrete*, V. 16, No. 3, pp. 366-380.

Bentz, E. C., Vecchio, F. J. and Collins, M. R., 2006, "Simplified modified compression field theory for calculating shear strength of reinforced concrete elements," *ACI Structural Journal*, V. 103, No. 4, Jul-Aug, pp. 614-624.

Canadian Standards Association, 2004, "CSA A23.3-04: Design of concrete structures," 240 pp.

CEB-FIP, 1993, "Model Code 1990," European Concrete Committee and International Federation for Prestressing, Lausanne, Switzerland.

CEN, 2005, "Eurocode 2: Design of Concrete Structures - Part 1-1 General Rules and Rules for Buildings. NEN-EN 1992-1-1:2005," Comité Européen de Normalisation, Brussels, Belgium, 229 pp.

Collins, M. P., Mitchell, D., Adebar, P. and Vecchio, F. J., 1996, "A general shear design method," *ACI Structural Journal*, V. 93, No. 1, Jan-Feb, pp. 36-45.

Collins, M. P., Bentz, E. C., Quach, P. T. and Proestos, G. T., 2015, "The Challenge of Predicting the Shear Strength of Very Thick Slabs," *Concrete international*, V. 37, No. 11, pp. 29-37.

Collins, M. R., Bentz, E. C. and Sherwood, E. G., 2008, "Where is shear reinforcement required? Review of research results and design procedures," *ACI Structural Journal*, V. 105, No. 5, Sep-Oct, pp. 590-600.

Falbr, J., 2011, "Shear redistribution in solid concrete slabs," MSc. Thesis, Delft University of Technology, Delft, pp. 151.

fib, 2012, "Model code 2010: final draft," International Federation for Structural Concrete; Lausanne, 676 pp.

fib Task Group on Utilisation of Concrete Tension in Design, 2001, "Punching of structural concrete slabs," fib, 314 pp.

Gardner, N. J., 2011, "Verification of Punching Shear Provisions for Reinforced Concrete Flat Slabs," *ACI Structural Journal*, V. 108, No. 5, pp. 572-580.

Gastebled, O. J. and May, I. M., 2001, "Fracture mechanics model applied to shear failure of reinforced concrete beams without stirrups," *ACI Structural Journal*, V. 98, No. 2, pp. 184-190.

Hallgren, M., 1996, "Punching shear capacity of Reinforced High Strength Concrete Slabs," Ph.D. Thesis, Royal Institute of Technology, Stockholm, pp. 206.

Hanson, N. W. and Hanson, J. M., 1968, "Shear and Moment Transfer between Concrete Slabs and Columns," *Journal of the PCA Research and Development Laboratories*, V. 10, No. 1, pp. 2-16.

Hsu, T. T. C., 1996, "Towards a unified nomenclature for reinforced-concrete theory," *Journal of Structural Engineering*, V. 122, No. 3, pp. 275-283.

Kani, G. N. J., 1964, "The Riddle of Shear Failure and Its Solution," *ACI Journal Proceedings*, V. 61, No. 4, April, pp. 441-467.

Kinnunen, S. and Nylander, H., 1960, "Punching of Concrete Slabs without Shear Reinforcement," Stockholm; 112 pp.

König, G. and Fischer, J., 1995, "Model Uncertainties concerning Design Equations for the Shear Capacity of Concrete Members without Shear Reinforcement," *CEB Bulletin 224, Model Uncertainties and Concrete Barrier for Environmental Protection*, July, pp. 49-100.

Lantsoght, E. O. L., van der Veen, C. and Walraven, J. C., 2013, "Shear in One-way Slabs under a Concentrated Load close to the support," *ACI Structural Journal*, V. 110, No. 2, pp. 275-284.

Lantsoght, E. O. L., van der Veen, C., Walraven, J. and de Boer, A., 2015, "Experimental investigation on shear capacity of reinforced concrete slabs with plain bars and slabs on elastomeric bearings," *Engineering Structures*, V. 103, pp. 1-14.

Lantsoght, E. O. L., 2016, "Extended Strip Model: Effect of self-weight and size effect," Stevin Report 25.5-16-03, Delft University of Technology, 42 pp.

Lantsoght, E. O. L., van der Veen, C., de Boer, A. and Alexander, S., 2016a, "Bridging the gap between one-way and two-way shear in slabs," *ACI SP International Punching Symposium*, pp. 20.

Lantsoght, E. O. L., de Boer, A. and van der Veen , C., 2016b, "Modeling of symmetrically and asymmetrically loaded reinforced concrete slabs," *SEMC 2016*, Cape Town, South Africa, pp. 6.

Lantsoght, E. O. L., van der Veen, C., de Boer, A. and Alexander, S. D. B., (in review), "Extended Strip Model for Slabs under Concentrated Loads."

Lantsoght, E. O. L., van der Veen, C., de Boer, A. and Walraven, J., in press, "Transverse Load Redistribution and Effective Shear Width in Reinforced Concrete Slabs," *Heron*, 29 pp.

Menétrey, P., 2002, "Synthesis of punching failure in reinforced concrete," *Cement & Concrete Composites*, V. 24, No. 6, pp. 497-507.

Moe, J., 1961, "Shearing strength of reinforced concrete slabs and footings under concentrated loads," Portland Cement Association Research and Development laboratories; Skokie, IL, 135 pp.

Muttoni, A. and Schwartz, J., 1991, "Behaviour of Beams and Punching in Slabs without Shear Reinforcement," *IABSE colloquium on structural concrete*, pp. 703-708.

Muttoni, A., 2008, "Punching shear strength of reinforced concrete slabs without transverse reinforcement," *ACI Structural Journal*, V. 105, No. 4, pp. 440-450.

Muttoni, A. and Ruiz, M. F., 2008, "Shear strength of members without transverse reinforcement as function of critical shear crack width," *ACI Structural Journal*, V. 105, No. 2, Mar-Apr, pp. 163-172.

Nielsen, M. P. and Hoang, L. C., 2011, "Limit analysis and concrete plasticity," 3rd ed. ed. CRC; Boca Raton, Fla.

Niwa, J., 1997, "Lattice Model with Concrete Tension Members for Shear Resisting Mechanism of Concrete Beams," *CEB Bulletin 237*, pp. 159-170.

Park, R. and Gamble, W. L., 2000, "Reinforced concrete slabs," 2nd ed. Wiley; New York, 716 pp.

Regan, P. E., 1982, "Shear Resistance of Concrete Slabs at Concentrated Loads close to Supports," Polytechnic of Central London, London, United Kingdom, 24 pp.

Reineck, K.-H., Bentz, E. C., Fitik, B., Kuchma, D. A. and Bayrak, O., 2013, "ACI-DAfStb Database of Shear Tests on Slender Reinforced Concrete Beams without Stirrups," *ACI Structural Journal*, V. 110, No. 5, pp. 867-876.

Reineck, K. H., 2010, "Strut-and-tie models utilizing concrete tension fields," *3rd fib International Congress*, Washington DC, USA, pp. 1-12.

Rombach, G. and Latte, S., 2009, "Shear Resistance of Bridge Decks without Transverse Reinforcement," *Beton- und Stahlbetonbau*, V. 104, No. 10, pp. 642-656.

Sagaseta, J., Muttoni, A., Ruiz, M. F. and Tassinari, L., 2011, "Non-axis-symmetrical punching shear around internal columns of RC slabs without transverse reinforcement," *Magazine of Concrete Research*, V. 63, No. 6, pp. 441-457.

Schlaich, J., Schafer, K. and Jennewein, M., 1987, "Toward a Consistent Design of Structural Concrete," *Journal Prestressed Concrete Institute*, V. 32, No. 3, pp. 74-150.

Valdivieso, D., Lantsoght, E. O. L. and Sanchez, T. A., 2016, "Effect of torsion on shear capacity of slabs," *SEMC 2016*, Cape Town, South Africa, pp. 6.

Vecchio, F. J. and Collins, M. P., 1986, "The Modified Compression-Field Theory for Reinforced-Concrete Elements Subjected to Shear," *Journal of the American Concrete Institute*, V. 83, No. 2, Mar-Apr, pp. 219-231.

1 Walraven, J. C., 2007, "Fracture mechanics of concrete and its role in explaining structural behaviour,"
2 *Fracture Mechanics of Concrete and Concrete Structures, Vols 1-3*, V. 1-3, pp. 1265-1275.
3 Wei, X., 2008, "Assessment of real loading capacity of concrete slabs," MSc. Thesis. Delft University of
4 Technology. 112 pp.
5